Full Paper

IMPACT OF TREE DENSITY ON SHORT RANGE VHF RADIO WAVE PROPAGATION IN THE MANGROVE SWAMP FOREST

F.O. Agugo
Nigerian Army School of Signals, Apapa, Lagos.

S.A. Adeniran
Department of Electronic and Electrical Engineering, Obafemi Awolowo University, Ile- Ife.
sadenira@oauife.edu.ng

O. Erinle
Department of Electronic and Electrical Engineering, Obafemi Awolowo University, Ile- Ife.

ABSTRACT

Propagation models are developed to suit particular applications and environments. Characterization of a forested radio channel for short range VHF/UHF communication with near ground antennas needs to consider all possible radio wave reflections - tree trunks, ground and tree canopy reflections - in addition to the foliage absorption effects of propagation through tree groves. In the mangrove forest where tree density is usually high, the capacity of tree elements for radio wave scattering at certain propagation parameters cannot be overlooked. This study used an integration of stochastic and empirical modelling to show that forest tree density is the most important parameter in path loss prediction in the mangrove at certain combat communication parameters.

1. INTRODUCTION

Short and medium range military communication/surveillance systems operate on near ground radio channels where radio propagation is highly affected by ecological factors. The new and indeed future wireless systems require that channels be characterized to greater details for optimal performance of wireless communication/surveillance networks. The aim of this study is to provide information on the radio propagation characteristics of the mangrove swamp forest at combat net parameters of near-ground antenna, VHF ranges of 30 - 80 MHz and 150 - 250 MHz and distance range of 50 - 300 metres.

It was obvious from (Meng et al., 2010) that any characterization of a forested radio channel for short range VHF/UHF communication with near ground antennas needed to consider all possible reflections - tree trunks, ground and tree canopy reflections as shown in Fig 1 - in addition to the foliage absorption effects of propagation through tree groves.

A propagation loss model that is based on the summation of the foliage loss (obtained from common foliage loss models) and the effects of radio wave reflections such as ground reflection and tree-canopy reflection was presented in (Meng et al., 2010). It was shown to give better accuracy for near ground VHF communication at short distance, when compared to commonly used Wiessberger, ITU-R and COST235 Models. The theoretical bases of this study are similar to the integration model which was proposed in (Meng et al., 2010) and used in (Agugo and Adeniran, 2011); however, the new insight in this study is the fact that the structure and high tree density of the mangrove forest cannot be taken as smooth flat terrain especially at short ranges and VHF or UHF frequencies (see Fig. 2), hence it cannot be assumed that it would produce only specular reflections as done in (Meng et al., 2010; Agugo and Adeniran, 2011).

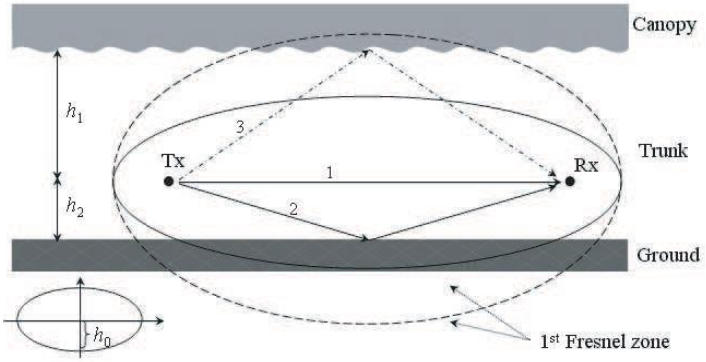

Fig. 1. Ray tracing geometry of direct-1, ground-reflected-2 and tree-canopy-reflected-3 waves (Meng et al., 2010).

Fig. 2: Photographs of Mangrove Swamp Forest.

This new insight is based on the results of the field measurements that were included in (Agugo and Adeniran, 2011),

which gave such interesting indications regarding the mangrove forest.

Essentially, the objective of this study was achieved through the analysis of terrain data and the received signal strength at selected distances from the transmitter of a wireless link that was operated at the combat net parameters of interest. Preliminary information on the forest composition and structure was used to determine significance of each of the dominant propagation mechanisms or phenomena in such channel at short-range, near-ground VHF band. The contribution of each significant mechanism to path loss was evaluated using stochastic geometrical optics approach and relevant standard empirical models. The mathematical formulation that sums the contributions of all the significant propagation mechanisms to obtain the total path loss was used as the characteristic equation or path loss model. This characteristic equation or model elicited the kinds of terrain data required for its quantitative evaluation. Field measurements were be conducted at two mangrove forest sites, first to obtain the primary terrain data required for estimating the quantitative value of path loss using the model, and secondly to obtain the actual values of path loss in the selected sites at the radio parameters of our interest. Measurement sites were selected to ensure difference in forest tree density. Secondary terrain data was obtained from literature as necessary. Graphs of path loss variability with respect to distance and frequency for different tree density values plotted with both the estimated and the measured values was analysed and compared to obtain their general trends and relationship. Estimation error of the model was calculated using statistical deviation method.

2. CONCEPTUAL FRAMEWORK

Generally, the basic propagation phenomena that are often considered in propagation modelling are reflection, refraction, diffraction, absorption and scattering (Zwick et al., 2009). A pictorial overview of these phenomena is shown in Fig 3.

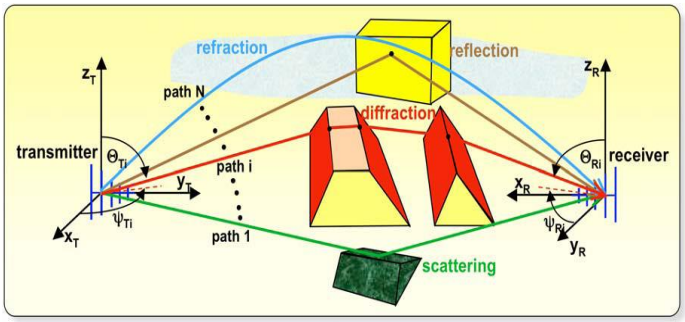

Fig. 3: Radio Propagation Phenomena.

Scattering is a phenomenon in which the direction or polarization of the wave is changed when the wave encounters propagation medium discontinuities in the order of or smaller than the wavelength. Scattered waves are produced by rough surfaces, small objects (e.g. foliage, street signs, etc) or by other irregularities in the channel as shown in Figs. 4 and 5. It results in a disordered or random change in the incident energy distribution. The actual received signal in a radio system is often different from what is predicted by free-space propagation, reflection, and diffraction models alone. Indeed, a wave propagating through a volume containing many individual small objects (e.g. forest), looses energy due to phase shifts and the non-vanishing imaginary part of the objects' total permittivity, as well as scattering off the direction of propagation. However, when an electromagnetic wave impinges on a single object whose size is small compared to the wavelength, a rough surface, or a volume containing many individual small objects such as tree trunks, branches, and leaves in a forest, the energy is spread out in all directions due to scattering, and this may even provide additional radio energy at the receiver (Zwick, 2009).

Hence, a theoretical description of these effects is very complex, and is thus mostly based on approximations. Therefore, losses relating to scattering are often accounted for by using simple empirical formulas.

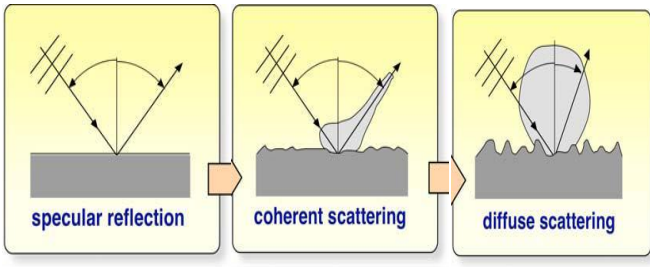

Fig. 4: Illustration of the transition from Specular Reflection to Scattering.

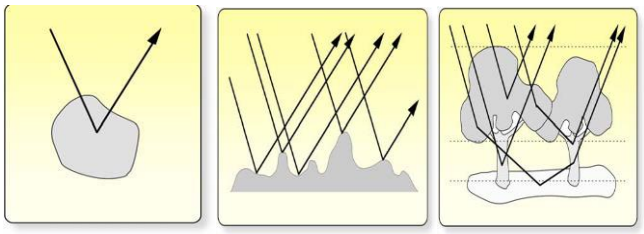

Fig. 5: Illustration of Point, Area and Volume Scattering.

The Blaunstein's model is a stochastic approach to investigate the absorbing and multiple scattering effects that accompany the process of radio wave propagation through forested areas (Blaunstein et al., 2003; Blaunstein and Christodoulou, 2007). This is a combination of probabilistic and deterministic approaches, which describes the random media scattering phenomenon. The geometrical optics approximation is used to account for propagation over a series of trees modelled as absorbing amplitude/phase screens with rough surfaces. A completely stochastic approach would require the propagation designer to obtain the absorption effects of trees using their real physical parameters, such as permittivity and conductivity, as well as the random distribution of their branches and leaves, which would be highly complex. However, it has been shown that it is possible to obtain reasonably accurate estimates of the absorption effects of trees using an appropriate standard empirical model such as the Weissberger's or ITU-R Models (Meng et al, 2010; Agugo and Adeniran, 2011). Hence, complex computations are eliminated without practical loss of accuracy by appropriate integration of empirical and stochastic models.

The Blaunstein's Model is a generalized model that covers wide ranges of frequency and distance. It gives the average total received EM field, I_{total}, in terms of the coherent and the incoherent components, I_{co} and I_{inc} respectively. The beauty of the model is that both I_{co} and I_{inc} are made up of terms some of which are relevant only for certain distance ranges, hence it can be adapted for particular distance ranges to reduce its complexity. In general, it evaluates the total path loss, L_{total}, as

$$L_{total} = -10 \log [\lambda^2 (I_{co} + I_{inc})] \quad (1)$$

The main limitation of Blaunstein's Model is in stochastic computation of absorption effects of trees. Nevertheless, its evaluation of the multiple scattering effects of trees shows high accuracy, and could be adapted especially where a reliable estimate of forest tree density is obtainable.

3. METHODOLOGY

A wave propagating through a volume containing many individual small objects (e.g. forest), looses energy due to phase shifts and the non-vanishing imaginary part of the objects' total permittivity, as well as scattering off the direction of propagation. However, an electromagnetic wave that impinges on a single object whose size is

small compared to the wavelength, a rough surface, or a volume containing many individual small objects such as tree trunks, branches, and leaves in a forest, would have the energy spread out in all directions due to scattering, and this may even provide additional radio energy at the receiver (Zwick et al., 2009). Hence, in addition to the absorptive effect, the multiple scattering effects of the mangrove trees need to be considered in evaluating the path loss in the mangrove forest at the propagation parameters of our interest.

To estimate the path loss resulting from the multiple scattering effects, we consider the array of trees as cylinders with randomly distributed surfaces, all placed on a flat terrain (Fig 6). Assuming that the reflecting properties of the trees are randomly and independently distributed (but are statistically the same), then the values of the reflection coefficient are complex with uniformly distributed phase in the range of [0, 2π], with correlation scales in the horizontal dimension, ℓ_h, and in the vertical dimension, ℓ_v, respectively. Thus, the average value of the reflection coefficients is zero, that is $\langle R(\varphi_s, r_s)\rangle = 0$. The geometry of the problem is shown in Fig. 7, where $A(d_1) = \mathbf{r}_1$ denotes the location of the transmitting antenna at height $h_T = z_1$; $B(d_2) = \mathbf{r}_2$ is the location of the receiving antenna at height $h_R = z_2$. To derive an average measure of field intensity for waves passing through the layer of trees after multiple scattering, we consider each tree as a phase-amplitude cylindrical screen. Figure 6 shows an array of these screens placed at $z = 0$. The trees have an average height, $\bar{h}$, and width, $\bar{w}$. These trees are randomly and independently distributed and they are oriented in arbitrary directions at the plane $z = 0$ with equal probability and with average density ν (per km^2). In near ground propagation where both antennas are placed within the forest environment and are lower than the average tree height, that is $0 < z_2; z_1 < \bar{h}$, then the multi-scattering effects are predominant and must be taken into account. In this case, the range of direct visibility (LOS conditions) between the two terminal antennas is given by $\bar{\rho} = {\gamma_0}^{-1}$, (Blaunstein and Christodoulou, 2007), where γ_0 is given as

$$\gamma_0 = 2\bar{w}\nu/\pi \tag{2}$$

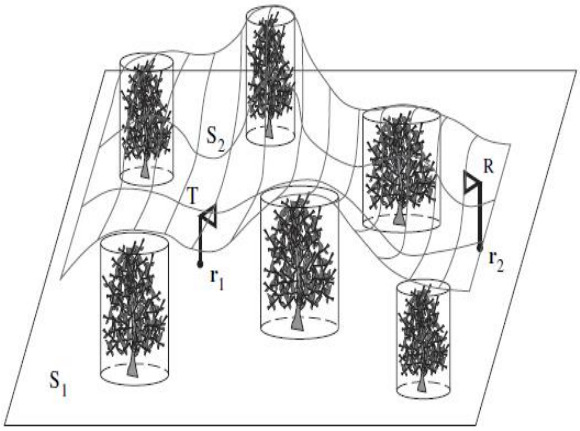

Fig. 6: Modelling of Trees as Cylindrical Screens.

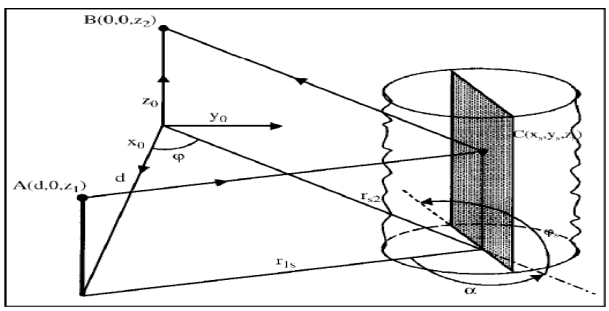

Fig. 7: Geometrical Presentation of the Scattering Model of Trees as Cylindrical Screens.

The 'roughness' of a tree's surface is described by considering it to have non uniform reflection coefficient, and introducing a correlation function for the reflection coefficient R. The correlation function is defined for $\ell_h, \ell_h, \ell_v \ll \bar{\rho}, \bar{w}, \bar{h}$ as

$$K(\mathbf{r}_{2S}, \mathbf{r}_{1S}) = \langle R_{2S} \cdot R^*_{1S}\rangle = R \cdot \exp\left\{-\frac{|\rho_{2S}-\rho_{1S}|}{\ell_h} - \frac{|z_{2S}-z_{1S}|}{\ell_v}\right\} \tag{3}$$

where $\mathbf{r}_{2S}$ and $\mathbf{r}_{1S}$ are points at the surface of an arbitrary tree as shown in Figure 2; R is the absolute value of the reflection coefficient given by Equation 8 for the two kinds of field polarization, $R_{2S} = R(\mathbf{r}_{2S}), R_{1S} = R(\mathbf{r}_{1S})$.

The main equations for the average field intensity are obtained by taking into account the Green's Function representation of wave propagation equation, Kirchhoff's approximation and Twersky's approximation. Green's Function representation of wave propagation describes an arbitrary source as a linear superposition of point sources. This is mathematically expressed as

$$s(\mathrm{r}) = \int \mathrm{d}\mathrm{r}'\, s(\mathrm{r}')\delta(\mathrm{r}-\mathrm{r}'). \tag{4}$$

The scalar wave equation with the source in the right hand side can be presented as

$$\nabla^2\Psi(\mathrm{r}) - k^2\Psi(\mathrm{r}) = s(\mathrm{r}) \tag{5}$$

and the corresponding equation for the Green's function in an unbounded medium is

$$\nabla^2\mathrm{G}(\mathbf{r},\mathbf{r}') - k^2\mathrm{G}(\mathbf{r},\mathbf{r}') = -\delta(\mathbf{r}-\mathbf{r}'). \tag{6}$$

The solution of equation (6) is (Blaunstein and Christodoulou, 2007)

$$\mathrm{G}(\mathrm{r}) = \frac{1}{4\pi}\frac{\exp\{ikr\}}{r} \tag{7}$$

and the corresponding solution of Equation 3.4 is

$$\Psi(\mathbf{r}) = -\int_{\mathrm{V}} \mathrm{d}\mathbf{r}'\mathrm{G}(\mathbf{r},\mathbf{r}')\, s(\mathbf{r}'). \tag{8}$$

Using Equation 3.6, we easily obtain a general solution for the inhomogeneous Equation (5) given by

$$\Psi(\mathbf{r}) = -\int_{\mathrm{V}} \mathrm{d}\mathbf{r}' \left\{\frac{\exp[ik|\mathbf{r}-\mathbf{r}'|]}{4\pi|\mathbf{r}-\mathbf{r}'|}\right\} s(\mathbf{r}'). \tag{9}$$

For the case of wave propagation through the forest layer with randomly distributed trees (screens), the total field at the receiver location $\mathbf{r}_2$ for the scattering problem can be written in the form

$$U(\mathbf{r}_2) = U_i(\mathbf{r}_2) + \int_S \left\{U(\mathbf{r}_s)\frac{\partial G(\mathbf{r}_2,\mathbf{r}_s)}{\partial \mathbf{n}_s} - G(\mathbf{r}_2,\mathbf{r}_s)\frac{\partial U(\mathbf{r}_s)}{\partial \mathbf{n}_s}\right\}\mathrm{d}S \tag{10}$$

where $U_i(\mathbf{r}_2)$ is the incident wave field, $\mathbf{n}_s$ is the vector normal to the terrain surface S at the scattering point r_s; $G(\mathbf{r}_2, \mathbf{r}_s)$ is the Green's function of the semi-space defined in Equations 3.6 and 3.8, which can be rewritten as (Blaunstein and Christodoulou, 2007)

$$\mathrm{G}(\mathbf{r}_2,\mathbf{r}_s) = \frac{1}{4\pi}\left\{\frac{\exp[ik|\mathbf{r}_2-\mathbf{r}_1|]}{|\mathbf{r}_2-\mathbf{r}_1|} \pm \frac{\exp[ik|\mathbf{r}_2-\mathbf{r}_1'|]}{|\mathbf{r}_2-\mathbf{r}_1'|}\right\}. \tag{11}$$

Here $\mathbf{r}_1'$ is the point symmetrical to $\mathbf{r}_1$ relative to the Earth's surface S_1. In integral Equation 9, the random surface S (relief of the terrain with obstructions) is treated as the superposition of an ideal flat ground surface S_1 ($z = 0$) and rough surface S_2 is created by the obstructions (see Figure 6). We construct the Green's function in the form of Equation 11 to satisfy a general electro-dynamic approach; that is, to describe both the vertical (sign "+" in Equation 11) and horizontal (sign "-" in Equation 11) polarizations with their corresponding boundary conditions. The boundary conditions (known as Dirichlet and Neumann's boundary conditions

respectively) are $\nabla G(\mathbf{r},\mathbf{r}')=0$ and $\mathbf{n}\cdot\nabla G(\mathbf{r},\mathbf{r}')=0$. In fact, by introducing the Green's function in Equation 11 with the "+" sign in Equation 10 we satisfy the Dirichlet boundary conditions at the flat (non disturbed) Earth's surface S_1 (z=0). That means, $G_{z=0}$ = 2 and $\frac{\partial U}{\partial \mathbf{n}_s}$= 0. At the same time, using the sign "-" we satisfy the Neumann boundary conditions at the plane z = 0: $G_{z=0}$ = 0 and u = 0. Hence, if the source is described by Equation 11, we can exclude the integration over the non disturbed surface S_1, assuming the surface S_1 is perfectly reflecting. Next, by using the Kirchhoff's approximation (which states that the wave at each point on a quasi smooth surface is a superposition of the incident and the reflected wave fields), we can determine the scattered field $U_r(\mathbf{r}_s)$ from the forested layer as a superposition of an incident wave $U_i(\mathbf{r}_2)$, the reflection coefficient $R(\varphi_s,\mathbf{r}_s)$, and the shadow function $Z(\mathbf{r}_2,\mathbf{r}_1)$. The shadow function equals one, if the point of scatter r_s inside the forested layer can be observed from both points $\mathbf{r}_1$ and $\mathbf{r}_2$ of the transmitter and receiver locations as shown in Figure 6, and equals zero in all other cases. Taking into account all these assumptions, Equation 10 can be rewritten following the method used by (Blaunstein et al., 2003) as

$$U(\mathbf{r}_2)=\mathrm{Z}(\mathbf{r}_2,\mathbf{r}_1)\tilde{G}(\mathbf{r}_2,\mathbf{r}_1)+2\int_{S2}\{\mathrm{Z}(\mathbf{r}_2,\mathbf{r}_s,\mathbf{r}_1)R(\varphi_s,\mathbf{r}_s)\cdot \tilde{G}(\mathbf{r}_2,\mathbf{r}_1)(\mathbf{n}_s\cdot\nabla_s)\}\mathrm{d}S, \quad (12)$$

where $\nabla_s=\left(\frac{\partial}{\partial x},\frac{\partial}{\partial y},\frac{\partial}{\partial z}\right)$, $\varphi_s=\sin^{-1}\left(\mathbf{n}_s\cdot\frac{\mathbf{r}_2-\mathbf{r}_1}{|\mathbf{r}_2-\mathbf{r}_1|}\right)$ (Figure 7) and $\tilde{G}(\mathbf{r}_2,\mathbf{r}_1)$ is the normalized Green's function. The solution of Equation 12 may be presented in operator form through a set of Green's functions expansion as (Blaunstein and Christodoulou, 2007; Blaunstein et al., 2003)

$$U_2=\mathrm{Z}_{21}\tilde{G}_{21}+\left(\mathrm{Z}_{2S}\hat{M}_{2S}R_S\right)\mathrm{Z}_{S1}\tilde{G}_{S1}+\left(\mathrm{Z}_{2S}\hat{M}_{2S}R_S\right)\left(\mathrm{Z}_{SS'}\hat{M}_{SS'}R_{S'}\right)\mathrm{Z}_{S'1}\tilde{G}_{S'1}+\cdots \quad (13)$$

Here, $\hat{M}_{\alpha\beta}$ is an integral-differential operator that describes the expression inside the bracket in Equation 13 and the variables $\mathrm{Z}_{\alpha\beta}$ and $R_{\alpha\beta}$ are the corresponding shadow and reflection coefficient functions denoted by indexes α and β. Noting Twersky's approximation, which states that the contributions of multiple scattered waves are additive and independent (hence does not take into account mutual multiple scattering effects) together with the condition that $\langle R(\varphi_s,d_s)\rangle=0$, it is possible to obtain the coherent part of the total field from Equation 13 by averaging Equation 12 over the reflecting properties of each tree and over all tree positions (Twersky, 1967). Thus,

$$\langle U_2\rangle=\langle \mathrm{Z}_{21}\rangle\tilde{G}_{21}. \quad (14)$$

Z_{21} is the "shadowing" function that describes the probability of existence of some obstructions in the radio path of the two terminal antennas. As the contributions of the multi-scattered waves are independent (Twersky, 1967), the coherent part of the total field intensity could be represented as (after averaging Equation 13) as

$$\langle I_2\rangle=\langle \mathrm{U}_2\cdot\mathrm{U}_2^*\rangle=\langle \mathrm{Z}_{21}\rangle\tilde{G}_{21}\cdot\tilde{G}_{21}^*ⁿ+\langle\left\{D_{2S,2\tilde{S}}+D_{2S',2\tilde{S}'}\cdot D_{SS',\tilde{S}\tilde{S}'}\right\}\cdot\mathrm{Z}_{S1}\cdot\mathrm{Z}_{\tilde{S}1}\cdot\tilde{G}_{S1}\cdot\tilde{G}_{\tilde{S}1}^*\rangle \quad (15)$$

where $D_{SS',\tilde{S}\tilde{S}'}=Z_{SS'}\cdot Z_{\tilde{S}\tilde{S}'}\cdot\hat{M}_{SS'}\cdot K_{S\tilde{S}}$.

For the conditions defined for the correlation function that describes the roughness of the tree surfaces, ℓ_h, ℓ_v, $\ll \bar{\rho},\bar{w},\bar{h}$ and $k\ell_h$, $k\ell_v \gg 1$ for $0<z_1<\bar{h}$, Equation 14 could be integrated over all the variables of the type $\Delta\mathbf{r}_S=\mathbf{r}_{\tilde{S}}-\mathbf{r}_S$ at the surfaces of scattering trees. By manipulating the expression in Equation 14 according to (Blaunstein and Christodoulou, 2007; Blaunstein et al., 2003), we obtain

$$\langle I_2\rangle=\langle \mathrm{Z}_{21}\rangle\left|\tilde{G}_{21}\right|^2+\langle\{Q_{2S1}+Q_{2S'S}\cdot Q_{SS1}+\cdots\}\cdot\mathrm{Z}_{S1}\left|\tilde{G}_{S1}\right|^2\rangle \quad (16)$$

Where $Q_{SS',\tilde{S}\tilde{S}'}=Z_{SS'}\cdot\left|\tilde{G}_{21}\right|^2\cdot\sigma_{S''S'S}$.

The cross-sectional area of scattering has been given as (Blaunstein and Christodoulou, 2007; Blaunstein et al., 2003)

$$\langle\sigma\rangle=\frac{\gamma_0 R}{4\pi}\cdot\sin^2\frac{\alpha}{2}\cdot\frac{k\ell_v}{1+(k\ell_v)^2(\sin\vartheta'-\sin\theta')^2}\cdot\frac{k\ell_h}{1+(k\ell_h)^2} \quad (17)$$

By averaging Equation 15 over all tree (screen) positions – integrating over the surfaces of the screens as well as over their mirror surfaces $(-\bar{h}\le z,z',z'',\ldots\le\bar{h})$. The averaging over the screen orientations for each scatter point affects only the value of σ from Equation 17. At the same time, the averaging over the number and position of all screens affects the "shadow" function Z. This approximation together with that of $\langle R(\varphi_s,r_s)\rangle=0$ (that the mean reflection coefficient round the tree is zero) makes it possible to obtain the coherent part of total field intensity, I_{co}, as (Blaunstein and Christodoulou, 2007; Blaunstein et al., 2003)

$$I_{co}=\frac{e^{-\gamma_0 d}}{16\pi^2 d^2}*\left[2sin\frac{kh_T h_R}{d}\right]^2 \quad (18)$$

For the incoherent part of the total field intensity, the Equation 15 can be presented in operator form as

$$\langle I_{inc}(\boldsymbol{r_2})\rangle=2\{Q+Q^2+Q^3+\cdots\}P(\boldsymbol{r_2},\boldsymbol{r_1}) \quad (19)$$

where the effect of the integral operator on the functions at the right-hand side of Equation 18 can be expressed as

$$Qf(\mathbf{r}_2,\mathbf{r}_1)=\int_V(\mathrm{d}\mathbf{r})P(\mathbf{r}_2,\mathbf{r})\frac{\langle\boldsymbol{\sigma}(\mathbf{r}_2,\mathbf{r},\mathbf{r}_1)\rangle}{|\mathbf{r}_2-\mathbf{r}_1|}f(\mathbf{r},\mathbf{r}_1). \quad (20)$$

The product $\mathrm{d}\mathbf{r}=\mathrm{d}S\cdot\mathrm{d}n$ defines the element of volume V of a plane parallel to the tree layer with width $,2\bar{w}$ over which the integration of the right hand side of Equation 20 takes place. Using the same assumptions that were used in deriving Equation 1 and setting $kz_2\gg1$, $z_2<\bar{h}$, we can integrate Equation 19 over variable z to get

$$(4\pi)^2|\rho_2-\rho_1|\cdot\langle I_{inc}(\boldsymbol{r_2})\rangle=2\{q+q^2+q^3+\cdots\}g(\rho_2-\rho_1) \quad (21)$$

where

$$g(\rho_2-\rho_1)=\frac{\exp\{-\gamma_0|\rho_2-\rho_1|\}}{|\rho_2-\rho_1|} \quad (22)$$

If the integration is over ρ with infinite limits, the operator $\hat{q}$ becomes

$$\hat{q}f(\rho_2,\rho_1)=\frac{v\cdot\bar{w}\cdot R}{4\pi}\int(\mathrm{d}\rho)\left[1-\frac{\rho_2-\rho}{|\rho_2-\rho|}\cdot\frac{\rho-\rho_1}{|\rho-\rho_1|}\right]g(\rho_2-\rho_1)f(\rho-\rho_1). \quad (23)$$

An evaluation of Equation 21, taking into account Equations 22 and 23 and using Laplace's method for $\gamma_0\rho\gg1$ yields the incoherent part of the total field intensity as

$$\langle I_{inc}(\boldsymbol{r_2})\rangle\approx\frac{\gamma_0 R}{(4\pi)^2}\left[\frac{R^3}{4(8)^3}\frac{\exp\{-\gamma_0 d\}}{d}+\frac{R}{32}\left(\frac{\pi}{2\gamma_0}\right)^{1/2}\frac{\exp\{-\gamma_0 d\}}{d^{3/2}}+\frac{1}{2\gamma_0}\frac{\exp\{-\gamma_0 d\}}{d^2}\right] \quad (24)$$

The first two terms in Equation 24 are important only at long distances $d>d_k=\frac{8^3}{\pi\gamma_0 R^2}$, whereas the third term is important at close ranges (Blaunstein and Christodoulou, 2007). Therefore,

$$I_{inc}=R_{HP,VP}*\frac{1}{32\pi^2 d^2}*e^{-\gamma_0 d} \quad (25)$$

provided that $d<\frac{8^3}{\pi\gamma_0 R^2}$.

Hence the path loss due to the multiple scattering effects of the mangrove tree elements, L_{MSE}, may be obtained by applying Equation (1) as

$$L_{MSE} = -10 \log [\lambda^2 (I_{co} + I_{inc})] \quad (26)$$

Similarly, the loss due to the absorptive effects, L_{AE}, is obtained using an appropriate standard empirical forested path loss model. Weissberger's Model is most suitable in the mangrove swamp medium (Meng et al, 2010; Agugo and Adeniran, 2011). Hence the characteristic equation or path loss model (referred hereafter as MIM), would evaluate the total path loss L_{MIM}, as the summation of L_{MSE} and L_{AE}, that is,

$$L_{MIM} = L_{MSE} + L_{AE}, \quad (27)$$

where L_{AE} is obtained using Weisberger's Model.

4. EVALUATION AND ANALYSIS OF RESULTS

In evaluating the path loss using MIM, an estimate of the tree density v, in the area of investigation is required. The value v is used with the average tree width w, to obtain the working average value of γ_0, which is a critical in the MIM model. This estimate of v (which is the number of trees per km^2) was obtained by simple proportion after getting the estimate of the number of trees in an area of 100 m^2, 500 m^2 or 1000 m^2 (whichever was more expedient at each measurement site). The number of trees can be (and indeed was in our case) obtained by physical enumeration. In Ilado-Odo for instance, the number of trees counted within some sampled small strips of forest 10m x 50m dimension ranged between 12 and 13 trees. Thus v could be evaluated as follows:

Average number of tree in the area of 500m^2 = 12.5; therefore, for an area of 1 km^2 (1000000 m^2), $v = \frac{12.5}{500} * 1000000 = 25000$ trees/km^2.

From the study, the tree density v was found to range between 25,000 and 32,000 per km^2, generally increasing from Lagos eastwards. Table 1 shows the values of γ_0 based on various values of the forest parameters estimated for specific mangrove forest areas.

Table 1: Average Values of Tree width and Density across the Nigerian Mangrove Belt

w (m)	v (km^{-2})	γ_0 (km^{-1})	Corresponding Areas
0.7	25,000	11.14	Lagos/Ogun
0.9	27,000	15.50	Ogun/Ondo
1.0	27,000	17.20	Cross Rivers/Akwa-Ibom
1.2	30,000	22.92	Delta/Rivers
1.3	30,000	24.83	Detla/Bayelsa
1.4	32,000	28.52	Bayelsa outskirts
1.5	32,000	30.56	Bayelsa Central

Note: w = Average tree width, v = numbers of tree per km^2, $\gamma_0 = 2\bar{w}v/\pi$.

The average tree width, w, ranges from 0.7 m to 1.5 m. (Note that the proper unit for w should be km, as the dimension of γ_0 is km^{-1}). The absolute reflection coefficient R for wood obtained is 0.4 (Blaunstein, 2004). The plots showing the variability of average path loss relative to distance are in Fig.8. Also, a normalized meshed graph of path loss variability relative to distance and tree density is shown in Fig. 9.

It is observed that the values of path loss at Ilado-Odo are generally lower than those of Nembe. This is in agreement with the prediction results of the MIM, which indicates that path loss should increases with forest tree density. This is despite the more availability of tree canopies at Nembe than Ilado-Odo. Also, there is a general straight line regression with distance. It is also seen that there is essentially negative loss within 50 m of antenna separation, that is, a reduction from the free space attenuation values obtained from Friis' equation. This may be explained by the high contribution of both the coherent and incoherent wave fields since this range may have direct LOS path in addition to volume scattered wave that may produce back scattering effects. The back scattering phenomenon explains why the MIM predicts negative loss at certain propagation and forest parameters.

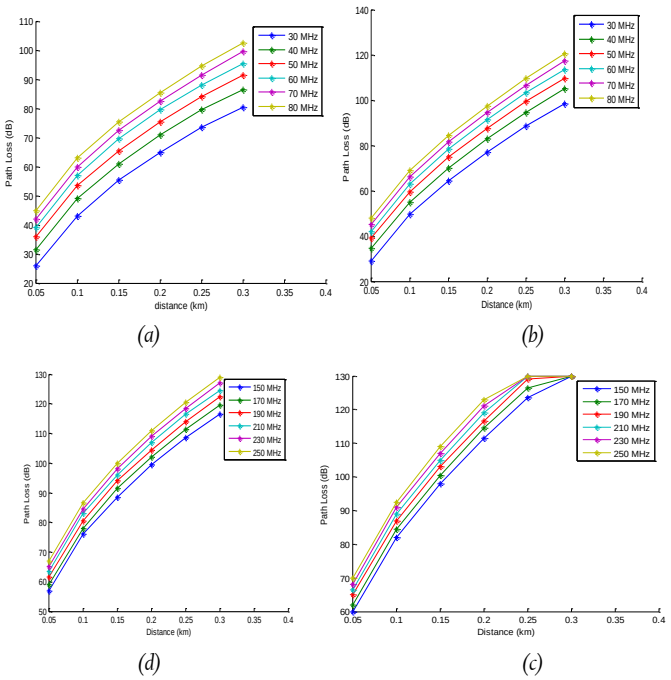

Fig 8: Graphs of average path loss against distance at given frequencies in (a) Ilado-Odo (b) Nembe (c) Ilado-Odo (d) Nembe.

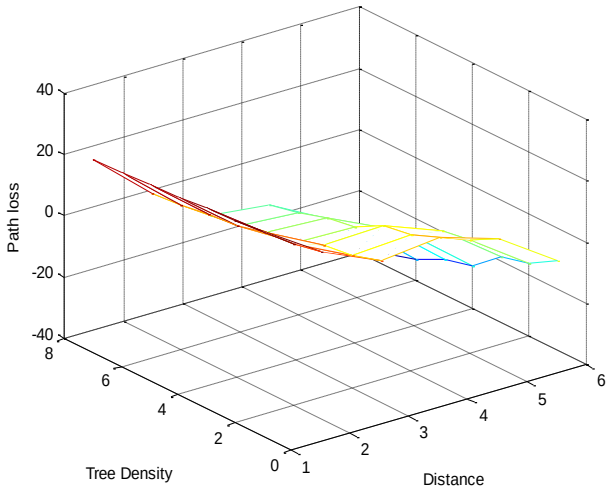

Fig. 9: Mesh Plot Showing Variability of Path loss with Distance and Tree Density (normalized).

4.1. Sensitivity analysis

It is possible to check the sensitivity of the prediction model to errors that may occur in any of the forest parameters required for path loss evaluation using the model. The accuracy of a theoretical prediction depends on the range of variance of each parameter, which describes the terrain features. For instance, a comparison of the values of path loss obtained in Ilado-Odo and Nembe indicates that variations in the values of $\gamma 0$ may have significant effect on LMSE, hence LMIM. From the values, it is seen that the variation of the tree densities within the range can affect the path loss by 10 - 20 dB. This is why, it is very important to know how accurate the various parameters should be, and what would be the effect of an error in any of the parameter i.e. average tree height, $\bar{h}$, width, $\bar{w}$, density v, and reflection coefficient R. For example, the value of R used in all the

predictions was 0.4. Deviations of this value over the range of ±50% (ΔR = 0.2) lead to deviations of the total path loss of less than ±1% (0.5 - 1.0 dB depending on the frequency and distance). Deviations of the parameter γ_0 in the range of ± 50% ($\Delta\gamma_0$ ≈ 5 for Lagos Area or 14 for Bayelsa Area) lead to deviations of the total path loss of in the range of ± 10 - 20% (7.0 - 15.0 dB). It is thus seen that MIM predictions are essentially sensitive only to errors in the value of γ_0. Since γ_0 depends mostly on the estimates of tree density ν per km^2, it can be generally concluded that the accuracy of the MIM largely lies on tree density estimates. Hence, the greatest care needs to be given to obtaining accurate estimates of tree density in the prediction of path loss in mangrove forests.

5. CONCLUSIONS

The combat net equipment/systems typically operate in the VHF and UHF bands, and are likely to be deployed with near ground antenna in areas where the forest structures provide them cover even from aerial view. The most significant contribution of this study was to show the prime importance of forest tree density in the estimation of radio propagation path loss in the mangrove swamp forest. This study has brought out interesting conclusions that would enhance the operation of smart military communication systems. These are:

i. Path loss predictions in the mangrove forest must take due consideration of forest tree density.
ii. The influence of specular ground and tree canopy reflections are negligible.
iii. Path loss variability with distance is approximately linear between 50-300m.
iv. The accuracy of path loss prediction is essentially dependent only on the accuracy tree density estimate.

REFERENCES

Agugo F. and Adeniran S., "Characterization of near-ground radio wave propagation in the mangrove and rain forest areas of Nigeria" Proceedings of 3rd IEEE international conference on adaptive science and technology, 249-255, 2011.

Blaunstein, N., I. Z. Kovacs, and Y. Ben-Shimol, "Prediction of UHF path loss for forest environments," Radio Sci., 38(3): 251-267, 2003.

Blaunstein, N., "Wireless Communication Systems," in Handbook of Engineering and Electromagnetics, Edited by R. Bansal, Chapter 12, Marcel Dekker, New York, pp. 417–481, 2004.

Blaunstein, N. and Christodoulou, C., "Radio Propagation and Adaptive Antennas for Wireless Communication Links: Terrestrial, Atmospheric and Ionospheric", John Wiley & Sons, Inc, 2007.

Meng, Y.S., Lee, Y.H. and Ng, B.C., "Path loss modelling for near ground VHF radio wave propagation through forest with tree canopy effect", *Progress in Electromagnetic research M*, Vol. 12, 2010.

Onuu, M. and Adeosun, A., "Investigation of Propagation Characteristics of UHF waves inAkwa-Ibiom State of Nigeria", Indian Journal of Radio and Space physics, 37:197-203, 2008.

Shoewu, O and Adedipe, A., "Investigation of radio waves propagation models in Nigerian rural and sub-urban areas," American Journal of Scientific and Industrial Research, Science, http://www.scihub.org/AJSIR, 2010.

Twersky, V., "Multiple scattering of electromagnetic waves by arbitrary configurations," Journal of Math. Phys., 8, 569-610, 1967.

Weissberger, M.A., "An initial critical summary of models for predicting the attenuation of radio waves by foliage," *ECAC- TR-81-101*, Electromagnetic Compatibility Analysis Centre, USA, 1981.

Zwick T. Younis, M., Adamiuk, G. and Balduaf, M., "Radio wave propagation fundamentals", Univeersitat Karlruhe (TH) Research University, 2009.